

15



16 Abstract

17 The spatial distribution of the attenuation of photosynthetic active radiation ($K_d(\text{PAR})$)
 18 was routinely estimated in China lakes and reservoirs. Higher mean value of $K_d(\text{PAR})$
 19 was observed in Northeastern plain and mountainous region (NER). A linear model is
 20 used to predict $K_d(\text{PAR})$, as a function of light absorption coefficient of pigment
 21 particulates (a_{phy}), colored dissolved organic matters (a_{CDOM}), and inorganic particulate
 22 matters (a_{NAP}): $K_d(\text{PAR}) = 0.41 + 0.57 \times a_{\text{CDOM}} + 0.96 \times a_{\text{NAP}} + 0.57 \times a_{\text{phy}}$ ($R^2 = 0.87$, $n = 741$,
 23 $p < 0.001$). Spatial $K_d(\text{PAR})$ was relatively dependent on the inorganic particulate
 24 matters (average relative contribution of 57.95%). When only consider the contribution
 25 of absorption of a_{OACs} to $K_d(\text{PAR})$, the results found that the a_{OACs} could explain 70%-
 26 87% of $K_d(\text{PAR})$ variations. In the lakes with low TSM concentration and non-
 27 eutrophic lakes with high TSM, a_{CDOM} was the most powerful predicting factor on
 28 $K_d(\text{PAR})$. In eutrophic lakes with high TSM, a_{NAP} had the most significant impact on
 29 $K_d(\text{PAR})$. This study allowed $K_d(\text{PAR})$ to be predicted from a_{OACs} values in the inland
 30 waters. Besides, results of this study are suggesting that new studies on the variability
 31 of $K_d(\text{PAR})$ in inland waters must consider the hydrodynamic conditions, trophic status
 32 and the distribution of optically active components within the water column.

33 **Keywords:** light attenuation, light absorption, optically active components,
 34 photosynthetic active radiation, inland waters

35



1. Introduction

Light is one of the most important factors governing primary production and photosynthesis in the aquatic ecosystems (Kirk, 1994; Ma & Song & Wen & Zhao & Shang & Fang & Du, 2016; Song & Ma & Wen & Fang & Shang & Zhao & Wang & Du, 2017). Light availability plays a crucial role in the distribution of phytoplankton and hydrophytes, and it is also a good indicator of the trophic state of an aquatic system. Photosynthetically active radiation (PAR) for phytoplankton growth is a product of the input of solar radiation at the surface and its reduction by optically active compounds (OACs) through absorption and scattering (Devlin & Barry & Mills & Gowen & Foden & Sivyer & Greenwood & Pearce & Tett, 2009). The diffuse attenuation of photosynthetic active radiation ($K_d(\text{PAR})$) is commonly used to quantitatively assess the light availability, it indicates the ability of solar radiation to penetrate a water column (Kirk, 1994). $K_d(\text{PAR})$ can be obtained by the profile of PAR values measured at different water depths according to Lambert-Beer's law (Devlin et al., 2009; Devlin & Barry & Mills & Gowen & Foden & Sivyer & Tett, 2008; Shi & Zhang & Liu & Wang & Qin, 2014). However, in situ measurements of $K_d(\text{PAR})$ in waters have obvious limitations, and it is difficult to achieve spatial coverage. Satellite remote sensing has achieved the mapping of $K_d(\text{PAR})$ distribution from various types of satellite remote sensing data in open sea, coastal and inland waters in recent years (Chen & Zhu & Wu & Cui & Ishizaka & Ju, 2015; Shi et al., 2014; Song et al., 2017). However, Environmental change and anthropogenic activity have made it challenging to accurately assess K_d patterns in the extremely turbid inland waters (Zheng & Ren & Li & Huang & Liu & Du & Lyu, 2016). The comprehensive analysis of the relationships between $K_d(\text{PAR})$ and a_{OACs} is an imperative requirement to retrieve $K_d(\text{PAR})$ from remote sensing data for turbid inland waters (Ma et al., 2016).



61 A number of components in water contribute to the attenuation of light, including
62 water itself, colored dissolved organic matters (CDOM), phytoplankton pigment
63 particles (expressed here as the concentration of chlorophyll-*a*), and inorganic
64 suspended particles. Water and CDOM absorb light, pigment and inorganic particles
65 absorb and scatter light (Effler, Schafran, and Driscoll, 1985; Shi et al., 2014).
66 Absorption and scattering by these OACs are the main attenuation factors of $K_d(\text{PAR})$
67 in the water (Budhiman & Suhyb Salama & Vekerdy & Verhoef, 2012; Zheng et al.,
68 2016). The relative contribution of OACs to $K_d(\text{PAR})$ have researched in numerous
69 studies previously in lakes, estuaries and offshore waters (Brandao & Brighenti &
70 Staehr & Barbosa & Bezerra-Neto, 2017; Lund-Hansen, 2004; Phlips, Lynch, and
71 Badylak, 1995; V-Balogh, Nemeth, and Voros, 2009; Yamaguchi & Katahira & Ichimi
72 & Tada, 2013), there is general agreement by now that inorganic suspended particles
73 had the decisive effect on light attenuation in turbid waters (Brandao et al., 2017; Yang
74 & Xie & Xing & Ni & Guo, 2005; Zhang & Zhang & Ma & Feng & Le, 2007a). In
75 transparent marine and freshwater systems, phytoplankton is also an important
76 component in PAR attenuation (Laurion & Ventura & Catalan & Psenner & Sommaruga,
77 2000; Lund-Hansen, 2004). Studies about $K_d(\text{PAR})$ partition and the influencing factors
78 provide important information to predict the underwater light climate from the
79 concentrations of these factors (Brandao et al., 2017; Zhang & Zhang & Ma & Feng &
80 Le, 2007c). In present, the contribution of OACs to light attenuation in many studies
81 included both OACs absorption (a_{OACs}) and particulates scattering. In fact, the
82 particulates scattering occupied small proportion of total contribution, most of the light
83 attenuation in water was induced by a_{OACs} (Belzile, Vincent, and Kumagai, 2002). Thus,
84 the relationship between $K_d(\text{PAR})$ and a_{OACs} is very essential to predict $K_d(\text{PAR})$ based
85 on a_{OACs} in inland waters.



86 Although $K_d(\text{PAR})$ characterization has been carried out in various aquatic
87 environments, including freshwater, estuaries, coastal water, and open ocean water
88 (Belzile et al., 2002; Cunningham, Ramage, and McKee, 2013; Frankovich, Rudnick,
89 and Fourqurean, 2017; Lund-Hansen, 2004; Zhang et al., 2007a), few studies have been
90 performed in the extremely turbid waters and plateau water with strong ultraviolet
91 radiation (Ma et al., 2016; Shi et al., 2014; Song et al., 2017). In transparent marine and
92 freshwater systems, phytoplankton was suggested to be an important component in light
93 attenuation (Brandao et al., 2017; Yang et al., 2005). However, in turbid inland waters,
94 the components of OACs vary independently (Matsushita & Yang & Yu & Oyama &
95 Yoshimura & Fukushima, 2015; Wen & Song & Zhao & Du & Ma, 2016), and studies
96 have pointed out that the components of OACs had large spatial and temporal variations
97 in turbid inland waters (Oliver & Collins & Soranno & Wagner & Stanley & Jones &
98 Stow & Lottig, 2017; Zhang & Zhou & Shi & Qin & Yao & Zhang, 2018; Zhao & Song
99 & Wen & Li & Zang & Shao & Li & Du, 2016). The governing factors controlling
100 $K_d(\text{PAR})$ always changed with the OACs concentration and component in different
101 inland waters (Brandao et al., 2017; Cunningham et al., 2013; Laurion et al., 2000).
102 China has a large number of inland waters, and they exhibit large variability in terms
103 of the optical properties and trophic status. A large proportion of lakes in China are
104 characterized by highly turbid waters (Song & Wen & Shang & Yang & Lyu & Liu &
105 Fang & Du & Zhao, 2018). Thousands of closed lakes with high salinity have developed
106 in the plateau area, and they are exposed to high intensity solar radiation (Laurion et al.,
107 2000; Ma & Yang & Duan & Jiang & Wang & Feng & Li & Kong & Xue & Wu & Li,
108 2011). To the best of our knowledge, there is little work has analyzed in detail the effect
109 of a_{OACs} on $K_d(\text{PAR})$ in a large variety of inland waters across China.

110 In this study, our objectives were (1) to describe the spatial distribution of $K_d(\text{PAR})$



111 in five limnetic regions, China; (2) evaluate which optical variables control the $K_d(\text{PAR})$
 112 in the water column of inland waters, especially in the different types of lakes, (3) to
 113 provide an empirical model to estimate $K_d(\text{PAR})$ in these inland waters. The study is
 114 essential to remote sensing of $K_d(\text{PAR})$ and evaluate the underwater light climate.

115 **2. Materials and Methods**

116 **2.1. Study area and Sampling description**

117 China is situated in eastern Asia, on the western shore of the Pacific Ocean, covering
 118 an area of approximately $9.6 \times 10^6 \text{ km}^2$ (E: $73^\circ 40' - 135^\circ 2' 30''$, N: $3^\circ 52' - 53^\circ 33'$). China
 119 is characterized by temperate continental climate, with a large temperature difference
 120 between summer and winter. The spatial distribution of annual average sunshine hours
 121 increases from southeast to northwest. There are a large number of lakes and reservoirs
 122 with the total surface area of $104,415 \text{ km}^2$, accounting for about 1.09% of the China
 123 total area, and this area accounts for 3.48% of the global lake and reservoir surface area
 124 (Ma et al., 2011; Raymond & Hartmann & Lauerwald & Sobek & McDonald & Hoover
 125 & Butman & Striegl & Mayorga & Humborg & Kortelainen & Duerr & Meybeck &
 126 Ciais & Guth, 2013; Wen & Song & Shang & Fang & Li & Lv & Lv & Chen, 2017).
 127 In accordance with the regions and topography, the lakes are divided into five limnetic
 128 regions: Inner Mongolia -Xinjiang plateau region (MXR), Tibet-Qinghai Lake Region
 129 (TQR), Northeastern plain and mountainous region (NER), Yunnan- Guizhou Plateau
 130 region (YGR), and Eastern plain region (ER) (Wen et al., 2017). Current estimation
 131 suggest that the total water storage of these lakes and reservoirs in China is about
 132 $1,280.75 \text{ km}^3$ (Song et al., 2018). The actual water storage of lakes in China is likely to
 133 be greater than currently known due to underestimation of the presence of many
 134 temporary small lakes (Song & Zang & Zhao & Li & Du & Zhang & Wang & Shao &
 135 Guan & Liu, 2013). The trophic status of lakes in China included oligotrophic,



136 mesotrophic, and hypereutrophic, water quality of the majority of lakes has degraded
137 (Jin, Xu, and Huang, 2005).

138 Surveys were carried out between April 2015 and September 2017 with a total of
139 741 locations covered 141 lakes and reservoirs in China (here after together called
140 lakes). A total of 13 field surveys covering the whole country was conducted. Details
141 about the distribution of the sampling lakes are shown in Figure 1. These lakes
142 distributed in different climatic zones with various land-use types. During the sampling
143 period the mean day air temperatures ranged from 15 to 25 °C. The areas of these lakes
144 ranged from 1 km² to 3,283 km², including freshwater and saline lakes. The surface
145 water (0.2-0.5 m depth) was collected in the acid-washed HDPE bottles, and were
146 placed in a portable refrigerator before they were carried back to the laboratory. The
147 location of each sampling station was recorded with a UniStrong G3 GPS. Water
148 samples were collected at 5-7 sampling stations from lakes on average, in the
149 meanwhile, PAR values were also measured in the same station. In total, PAR values
150 were collected in 741 stations in nine field experiments. The PAR values were
151 measured using the LI-COA 193SA underwater spherical quantum sensor. The
152 operation was conducted on the sunny side of the boat to avoid any shadow effects. The
153 PAR measurements were taken at no less than five point's depth for each station. At
154 each depth in the water, PAR value was continuously recorded for 15 s and output an
155 averaged value, the average value was regarded as the PAR value at this water depth
156 (Ma et al., 2016).

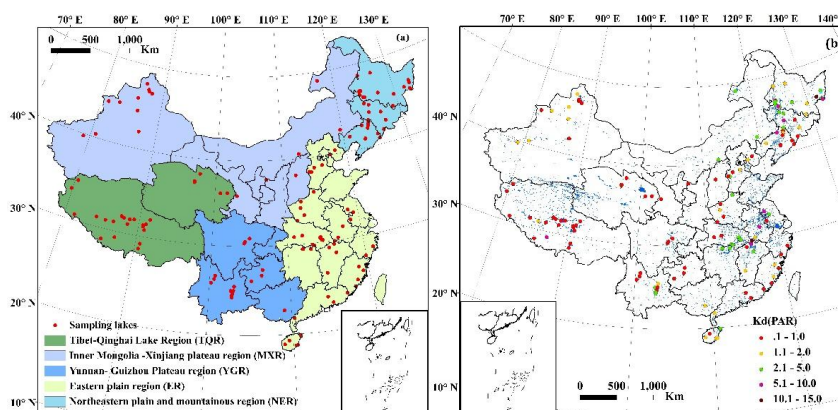


Fig. 1 Study area location and sampling lakes distribution, (a) sampling lakes distribution in five limnetic regions, (b) $K_d(\text{PAR})$ values distribution of every sampling lake

2.2. Water quality and light absorption parameters measurement

Salinity and pH were measured by a portable multi-parameter water quality analyzer (YSI 6600, U.S) in situ with the uncertainty of 0.01 ppt and 0.01, respectively. Secchi disk depth (SDD) at each sampling site was measured using a 30 cm diameter Secchi disk. All water samples were filtered through 0.45 μm mixed fiber millipore filters within 24 h of sampling, and the filtered waters were used to TN concentrations analysis by a continuous flow analyzer (SKALAR, San Plus System, the Netherlands). Total phosphorus (TP) was determined using the molybdenum blue method after the samples were digested with potassium peroxydisulfate (APHA, AWWA, and WEF, 1998). DOC concentrations were also analyzed using a total organic carbon analyzer (TOC-VCPN, Shimadzu), details can be found in the reference (Song et al., 2018). Chlorophyll a (*Chla*) was extracted from raw water samples using a 90% buffered acetone solution, and the concentration was determined by spectrophotometry (UV- 2600 PC, Shimadzu) (Jeffrey & Humphrey, 1975). Total suspended matter (TSM) concentration was determined gravimetrically, a certain volume of raw water were filtered through pre-combusted 0.7 μm glass fiber millipore filters (Whatman, GF/F 1825-047), the



176 particulate matter were retained in the filters, and then the filters were combusted for
177 2h on 400°C. TSM concentration was calculated by the difference between filtered
178 combusted filter and non- filtered combusted filter(Cleveland & Weidemann, 1993).

179 Total particulate light absorption (a_p) of the filter captured TSM was determined
180 by UV spectrophotometry (Shimadzu, 2660) with a virgin filter as a reference
181 (Cleveland & Weidemann, 1993). Then the sodium hypochlorite solution was used to
182 remove pigments in this filter, and the bleached filter was determined again to obtain
183 the optical density (OD_λ) of the non-algal particles (a_{NAP}). The pigment or
184 phytoplankton light absorption coefficient (a_{phy}) was the difference between a_p and a_{NAP} .
185 The collected water samples were filtered in turn through a GF/F 0.7 μ m glass fiber
186 membrane and a 0.2 μ m polycarbonate membrane to extract CDOM. The filtering
187 process should be finished within 24 h away from light. Light absorption of colored
188 dissolved organic matter (a_{CDOM}) in the waters was also measured using a UV-2600
189 spectrophotometer equipped a 5 cm quartz cuvette, the Milli-Q water was used as a
190 reference. The light absorption coefficient of CDOM at 700 nm was used to correct
191 CDOM absorption coefficients to eliminate the internal back scattering (Bricaud, Morel,
192 and Prieur, 1981). The absorption coefficients (a_p , a_{phy} and a_{CDOM}) were derived from the
193 measured OD_λ as the following equations (Bricaud et al., 1981; Bricaud & Stramski,
194 1990). In this study, absorption coefficients at 440 nm was chosen for analysis later in
195 this study (Wen et al., 2016). The light absorption of optically active components (a_{OACs})
196 is the sum of a_{CDOM} and a_p . Where $a_{CDOM}(\lambda)$, $a_p(\lambda)$, and $a_{phy}(\lambda)$ are the CDOM, total
197 particulate and phytoplankton absorption coefficients at a given wavelength,
198 respectively; L is the cuvette path length (0.01 m); S is the effective area of the deposited
199 particle on the fiber membrane (m^2); V is the volume of the filtered water (m^3); 2.303
200 is the conversion factor; and $OD_{(null)}$ is the OD value at 700 nm.



$$a_{CDOM}(\lambda) = 2.303 \times [OD_{(\lambda)} - OD_{(null)}] / L \quad (1)$$

$$a_p(\lambda) = 2.303 \times \frac{S}{V} \times OD_{(\lambda)} \quad (2)$$

$$a_{phy}(\lambda) = a_p(\lambda) - a_{NAP}(\lambda) \quad (3)$$

2.3. Data analysis

$K_d(\text{PAR})$ was calculated using the exponential regression model as the following equation, where Z is the water depth, and PAZ_Z is the photosynthetic active radiation value at depth Z (Pierson & Kratzer & Strombeck & Hakansson, 2008; Stambler, 2005). The results were accepted only if the coefficient of determination (R^2) was higher than 0.95.

$$\text{PAR}_{Z2} = \text{PAR}_{Z1} \times e^{-K_d(\text{PAR}) \times (Z_2 - Z_1)}$$

A classification regression tree approach (CHAID) was used to classify the lakes based on $K_d(\text{PAR})$ in SPSS 19.0. $K_d(\text{PAR})$ was used value as the response variable, the explanatory variables were TSM, Chla, a_{CDOM} , pH, salinity, and trophic status of lakes. Mean value and standard error of $K_d(\text{PAR})$ were calculated for each branch of the regression tree.

We approached data analysis in the following ways: First, the $K_d(\text{PAR})$ differences in different limnetic regions across China were quantified by the regional mean value of all lakes. Meanwhile, the relative contributions of a_{OACs} to $K_d(\text{PAR})$ was calculated according to the references (Brandao et al., 2017; Kirk, 1976; Pierson et al., 2008; Pope & Fry, 1997). The second approach was to establish links between $K_d(\text{PAR})$ and a_{OACs} in lakes using in situ measured values of all sampling sites. Third, regression tree analysis was used to classify the lakes based on $K_d(\text{PAR})$ values, and the relationships between $K_d(\text{PAR})$ and a_{OACs} in different types of lakes were explored using the multivariate regression analysis.

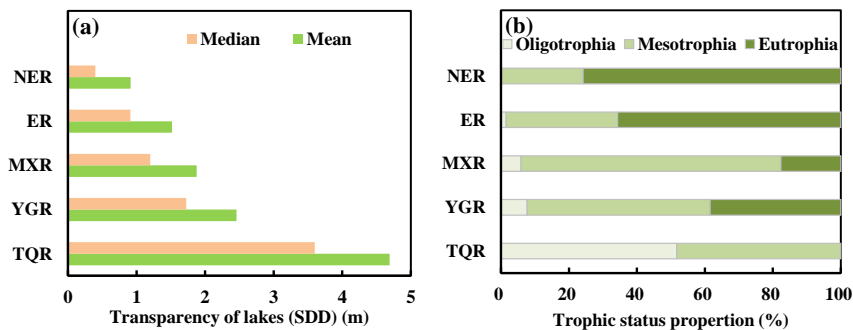


225 **3. Results**

226 **3.1 General surface water properties of lakes in different limnetic regions**

227 In all field surveys conducted over the 141 lakes across different limnetic regions
 228 interweaved with the diverse geographical environments, a large diversity of lakes with
 229 varying water qualities was encountered. We analyzed the transparency and trophic
 230 status of these lakes, and found that lakes in the YGR had the highest transparency,
 231 followed by YGR, MXR, ER, and NER showed the lowest transparency (SDD
 232 median/mean \pm standard deviation: 0.40/0.90 \pm 1.03 m) (Fig. 2a). The lakes in NER were
 233 highly turbid. NER is in the fluvial plains, the most of lakes in this area are shallow (2.8
 234 \pm 1.8 m) with re-suspension of bottom sediments. The trophic status of lakes across
 235 different limnetic regions showed that 24.14% studied lakes in NER had a mesotrophic
 236 status, and others were all eutrophic lakes (75.86%). The proportion of eutrophication
 237 of NER lakes was the highest in five limnetic regions, followed by ER (65.67%) (Fig.
 238 2b). Agricultural non-point pollution combined with industrial and domestic sewage
 239 discharge were the main reasons for these highly eutrophic waters in the NER and ER.

240 Compared with MXR, lakes in the YGR were more transparent (1.73/2.46 \pm 2.48
 241 m) (Fig. 2a). It is possible that most of the lakes in the YGR are deeper tectonic ones
 242 (average: 13.8 m). Lakes in the eastern part of Inner Mongolia were shallow, and strong
 243 wind caused re-suspension, resulting in the water turbidity. In these limnetic regions,
 244 most of lakes were mesotrophic (>50%), only a few lakes were oligotrophic (<10%)
 245 (Fig. 2b). Lakes from the TQR are usually tectonic origins with a larger water depth
 246 (21.7 \pm 16.8 m), they are more transparent (3.60/4.69 \pm 3.62 m). Because of less human
 247 activities and limited agricultural non-point pollution, the studied lakes in this regions
 248 did not show eutrophication, over half of the sampling waters were oligotrophic
 249 (51.72%), and others were all mesotrophic status (48.48%) (Fig. 2b).



250

251 Fig. 2 Analysis of transparency and trophic status of lakes in China's five limnetic regions. (a) the
252 transparency analysis; (b) trophic status analysis.

253 3.2 Spatial distribution of $K_d(\text{PAR})$

254 Due to the diverse geographical environments in the area of study, the sampled lakes
255 included the varying $K_d(\text{PAR})$ values (Fig. 1). $K_d(\text{PAR})$ values in different lakes ranged
256 from $0.11\text{--}13.93\text{ m}^{-1}$ with the mean of 1.99 m^{-1} . The minimum value occurred in the
257 Pumoyum Co Lake of the southern Tibetan Plateau region. The maximum value
258 occurred in the Qingnian reservoir of Northeastern region. The average $K_d(\text{PAR})$ value
259 for each of the five lake groups was calculated and ranged from 0.60 m^{-1} in TQR to
260 3.17 m^{-1} in NER (Fig. 3). In NER, the minimum value occurred in the Hengren reservoir
261 of 0.47 m^{-1} . In ER, the minimum value occurred in Haicang Lake of 0.20 m^{-1} . In MXR,
262 the minimum value occurred in Sayram Lake of 0.13 m^{-1} . In YGR, the minimum value
263 occurred in Fuxian Lake of 0.25 m^{-1} . In TQR, the minimum value occurred in Pumoyum
264 Co Lake of 0.11 m^{-1} .

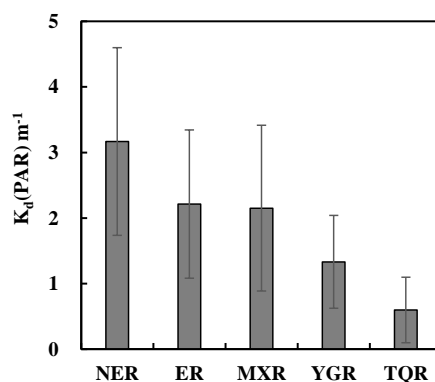
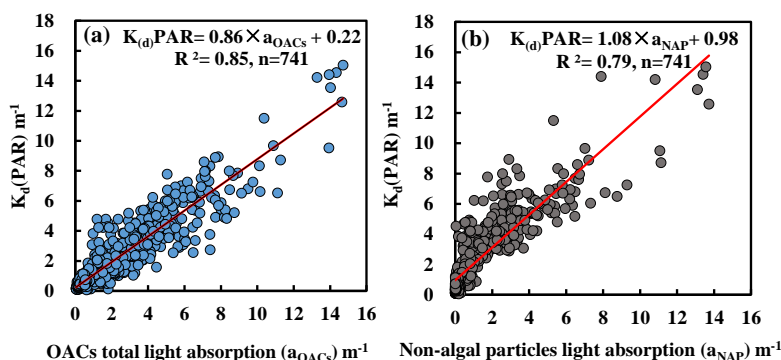
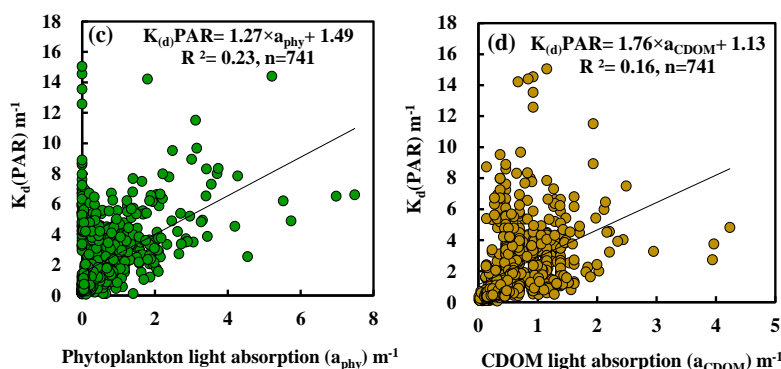


Fig. 3 Compare of mean $K_d(\text{PAR})$ values in five limnetic regions

3.3 Relationship between $K_d(\text{PAR})$ and OACs light absorption

A significant positive correlation was observed between $K_d(\text{PAR})$ and OACs total light absorption in lakes across China at all sampling sites, data were evenly distributed on both sides of the regression line (Fig. 4a). The best function to describe the relationship through a linear model: $K_d(\text{PAR}) = 0.86 \times a_{\text{OACs}} + 0.22$ ($R^2 = 0.85$, $n = 741$). The linking between $K_d(\text{PAR})$ and light absorption of each optically active compound was also explored. Except a_{NAP} showed a significant positive correlation with $K_d(\text{PAR})$ (Fig. 4b), they all had no significant linear relationship to $K_d(\text{PAR})$ (Fig. 4c-4d).





276
 277 Fig. 4 Scatter plots of diffuse attenuation vs light absorption of optically active components, (a)
 278 aOACs, (b) a_{NAP}, (c) a_{phy}, and (d) a_{CDOM}

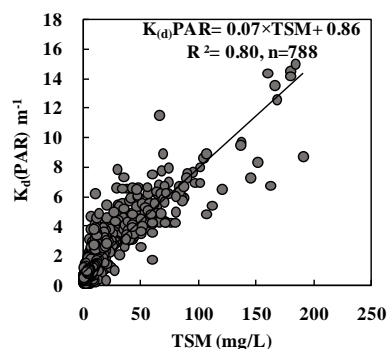
279 The result of multiple regression analysis showed that all the optically active
 280 components had impact on $K_d(\text{PAR})$, and the relational expression was as follow:
 281 $K_d(\text{PAR}) = 0.41 + 0.57 \times a_{\text{CDOM}} + 0.96 \times a_{\text{NAP}} + 0.57 \times a_{\text{phy}}$ ($R^2 = 0.87$, $n = 741$, $p < 0.001$) (Table
 282 1). The standardized coefficient of independent variables indicated that a_{NAP} had the
 283 most significant impact on $K_d(\text{PAR})$, followed by a_{phy}. TSM expresses the total
 284 concentration of inorganic and pigment particulate matter in water (Budhiman et al.,
 285 2012). The relationship between $K_d(\text{PAR})$ and TSM was also explored to support the
 286 regression analysis result (Fig. 5).

287 Table 1 Summary of multiple regression analysis

	R	R Square	Adjusted R Square	Std. Error of the Estimate	Sig.
All lakes	0.931	0.867	0.866	0.833	0.000
TSM <3.8 mg/L	0.863	0.744	0.742	0.220	0.000
TSM >3.8 mg/L (Non-eutrophic lakes)	0.880	0.774	0.770	0.429	0.000
TSM >3.8 mg/L (Eutrophic lakes)	0.874	0.764	0.762	1.106	0.000



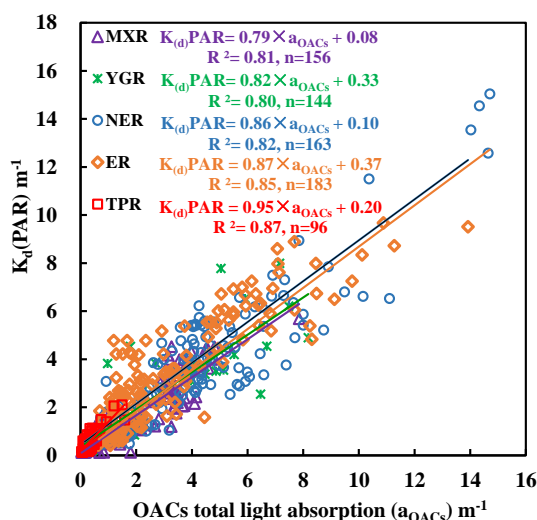
288 Dependent Variable: $K_d(\text{PAR})$; Predictors: constant, a_{phy} , a_{NAP} , a_{CDOM}



289

290 Fig. 5 Relationship between $K_d(\text{PAR})$ and total suspended matter concentration (TSM)

291 In five limnetic regions, the significant positive correlation was also observed
292 between $K_d(\text{PAR})$ and total light absorption of OACs (Fig. 6). The relationship
293 coefficient and fitting degree (R^2) all changed for lakes in different limnetic regions.
294 The regression model in TQR had the best fitting degree ($R^2 = 0.85$) and the greatest
295 relationship coefficient (slope=0.95) than in other limnetic regions. In MXR, the
296 regression model was $K_d(\text{PAR}) = 0.79 \times a_{\text{OACs}} + 0.08$ ($R^2 = 0.81$, $n = 156$) with the smallest
297 relationship coefficient. In YGR, the regression model was $K_d(\text{PAR}) = 0.82 \times a_{\text{OACs}} + 0.33$
298 ($R^2 = 0.80$, $n = 156$) with the lowest fitting degree.



299



Fig. 6 Relationships between $K_d(\text{PAR})$ and a_{OACs} in five limnetic regions

In all limnetic regions in this study, $K_d(\text{PAR})$ was dominated by inorganic particulate matter absorption/scattering, followed by pigment particulate matters in all limnetic regions with mean relative contributions of 57.95% and 28.20%, respectively. The highest mean relative contribution of inorganic particulate matter to $K_d(\text{PAR})$ (71.55 %) was in highest YGR, followed by NER (64.17 %), TQR (59.35 %), MXR (48.26 %), and ER (46.45 %) (Fig. 7). There is a little part of the $K_d(\text{PAR})$ variation could be explained by CDOM with the contributions in YGR of 6.78%, in NER of 9.99%, in TQR of 10.38%, in MXR of 11.75%, and in ER of 8.71% (Fig. 7).

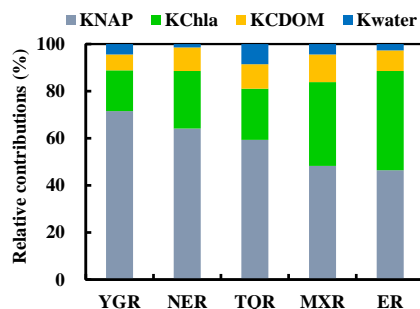


Fig. 7 Relative contributions of OACs to $K_d(\text{PAR})$. K_{water} is the partial attenuation coefficient by pure water, K_{CDOM} by CDOM, K_{NAP} by inorganic suspended particles, and K_{Chla} by pigment particles

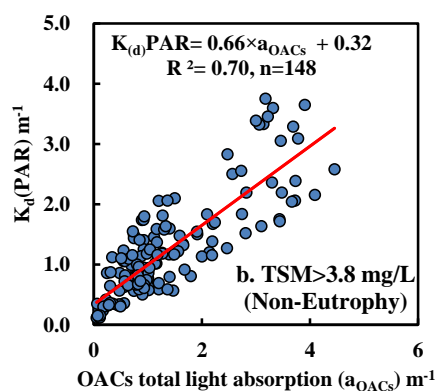
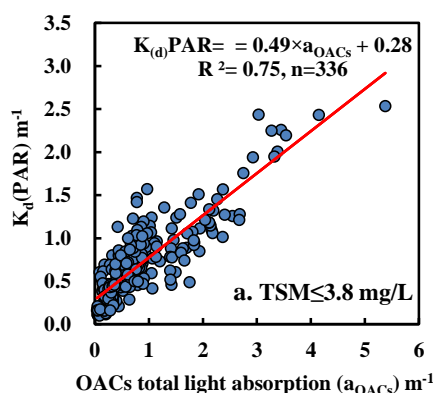
3.4 Relationship between $K_d(\text{PAR})$ and a_{OACs} in different lakes

Regression tree analysis showed this pattern of $K_d(\text{PAR})$ was mainly affected by TSM concentration in these inland lakes. The $K_d(\text{PAR})$ values in these lakes could be divided into two branches having a TSM threshold of 3.8 mg/L. When the TSM concentration of water was lower than 3.8 mg/L, the TSM concentration was the only predictive factor for $K_d(\text{PAR})$ values. However, the $K_d(\text{PAR})$ value in lakes with the TSM concentration higher than 3.8 mg/L, was also affected by trophic status. $K_d(\text{PAR})$ value in oligo- and Meso- trophic waters (mean \pm SD: $1.26\pm0.89 \text{ m}^{-1}$) was lower than in eutrophic waters



(mean \pm SD: 4.59 \pm 2.18 m⁻¹). From this point forward, the lakes are divided into two types used 3.8 mg/L TSM concentration as a threshold: low TSM lakes and high TSM lakes.

In order to specify the model applicability, the relationship between $K_d(\text{PAR})$ and a_{OACs} was also analyzed established for the lakes with different TSM concentration and trophic status. The regression model for lakes with low TSM had a lower slope (slope =0.49) than lakes with high TSM (slope =0.66, slope =0.73) with a good fitting degree (R^2) (Fig. 8). However, the relationship coefficient and R^2 all changed for lakes with different trophic status. In the oligo- and Meso- trophic waters (non-eutrophy), the R^2 attained 0.70 with the relationship coefficient 0.66 (Fig. 8). In the eutrophic waters, the regression model was $K_d(\text{PAR})=0.73 \times a_{\text{OACs}}+1.04$ with the R^2 of 0.72 (Fig. 8).



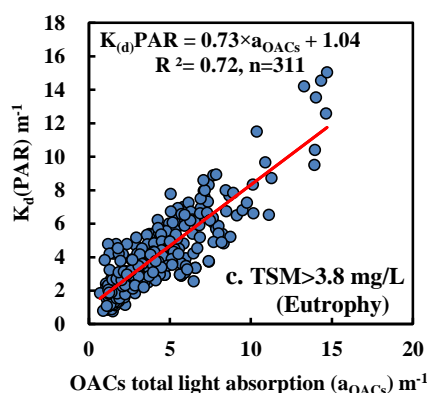


Fig. 8 Relationships between $K_d(\text{PAR})$ and a_{OACs} in different lakes

In the waters with low TSM, the result of multiple regression analysis showed a_{CDOM} had the most significant impact on $K_d(\text{PAR})$, followed by a_{NAP} , the relational expression was $K_d(\text{PAR}) = 0.30 + 0.48 \times a_{\text{CDOM}} + 0.72 \times a_{\text{NAP}} + 0.20 \times a_{\text{phy}}$ ($R^2 = 0.74$, $p < 0.001$) (Table 1). In the waters with high TSM, the multiple regression analysis indicated that not all the OACs had impact on $K_d(\text{PAR})$ in oligo- and Meso- trophic waters. a_{phy} was excluded during the building of regression model. The relational expression was as follow: $K_d(\text{PAR}) = 0.56 + 0.51 \times a_{\text{CDOM}} + 0.52 \times a_{\text{NAP}}$ ($R^2 = 0.77$, $p < 0.001$) (Table 1). The standardized coefficient of independent variables indicated that a_{CDOM} had more impact on $K_d(\text{PAR})$ than a_{NAP} in these non-eutrophic waters. In eutrophic waters with high TSM, the regression model was $K_d(\text{PAR}) = 1.47 + 0.35 \times a_{\text{CDOM}} + 0.82 \times a_{\text{NAP}} + 0.41 \times a_{\text{phy}}$ ($R^2 = 0.76$, $p < 0.001$) (Table 1). a_{NAP} had the most significant impact on $K_d(\text{PAR})$, followed by a_{phy} .

4. Discussion

4.1 $K_d(\text{PAR})$ in different limnetic regions of China

In the present study, 47.37% of the in situ $K_d(\text{PAR})$ values ranged from 0.11 m^{-1} to 1.00 m^{-1} , and 43.61% of $K_d(\text{PAR})$ ranged from 1.00 m^{-1} to 5.00 m^{-1} , reflecting that approximately half of these lakes are the turbid water body. The comparison of the



average $K_d(\text{PAR})$ value in the five limnetic regions indicated that the lakes in TQR were the most clear water, and the lakes in NER were the most turbid water (Fig. 3a). The lake area in TQR accounts for 51.4% of total China lake area, and the majority of TQR lakes are closed lakes with high salinity and low temperature (Ma et al., 2011; Song et al., 2018). The lacustrine environment in TQR is suffered less interference from anthropogenic activity with little allochthonous nutrient. The algae growth is few due to the high salinity, low temperature, and low nutrient input, accompanying with low Chla concentration. Moreover, the strong ultraviolet radiation in TQR could cause CDOM photolysis and photobleaching in waters, resulting in low CDOM absorption (Shang & Song & Wen & Lyu & Zhao & Fang & Zhang, 2018). Many large and medium-sized lakes in TQR, developed in intermontane basin or longitudinal valley, are the tectonic lake with deep water and steep shore. The TSM concentration in these deep lakes may be not significantly influenced by surface runoff and wind disturbance. According to the above reasons, the lakes in TQR may have a high water transparency, and the attenuation of light may be relatively few than other limnetic regions. Previous study has pointed out that most of lakes in NER were shallow lakes (Song et al., 2013), and in shallow lakes, TSM usually plays a noticeable impact on the attenuation of light and water transparency (Pierson, Markensten, and Strömbeck, 2003; Shi et al., 2014; Van Duin & Blom & Los & Maffione & Zimmerman & Cerco & Dortch & Best, 2001). TSM concentration is always higher in the shallow lakes due to the sediment re-suspension driven by wave disturbance (Shi et al., 2014). A lake's susceptibility to sediment re-suspension induced by wind-driven waves can be estimated by a dynamic ratio index of 0.8 km/m (the square root of the surface area divided by the average depth) (Bachmann, Hoyer, and Canfield, 2000). We calculated the dynamic ratios for the lakes in NER, results showed that the values ranged from 0.82 to 10.16 km/m. All lakes in



377 NER in this study exceeded the critical value, which supported that the resuspension
378 driven by winds happened in these NER lakes. The higher TSM concentration led to
379 the water turbidity and high $K_d(\text{PAR})$ value. These results were similar to those for
380 other shallow, turbid, inland waters (Shi et al., 2014; Song et al., 2017; Zheng et al.,
381 2016).

382 The $K_d(\text{PAR})$ in the water is determined by pure water and OACs, but the main
383 deciding factor may be different in different environments and lakes. The relative
384 contributions of OACs showed $K_d(\text{PAR})$ was dominated by inorganic particulate matter
385 absorption/scattering in all limnetic regions in this study (Fig. 7), the findings are
386 similar to previous findings on inland water bodies (Devlin et al., 2009; Ma et al., 2016;
387 Shi et al., 2014; Zhang et al., 2007a). However, there were marked regional differences
388 in the relative roles of inorganic particulate matter, Chl-*a* and CDOM to $K_d(\text{PAR})$ (Fig.
389 7). The highest relative contribution of inorganic particulate matter was presented in
390 YGR (Fig. 7). In this study, most of the studied lakes in the YGR are tectonic ones with
391 the mean deep more 10 m. The seasonal water layering is a universal phenomenon in
392 deep lakes (Ndebele-Murisa & Musil & Magadza & Raitt, 2014; Wetzel, 2001).
393 Previous studies have been demonstrated that mixing of the water column caused
394 resuspension of particulate matter increasing inorganic particulate matter
395 concentrations (James, Best, and Barko, 2004; Pierson et al., 2008; Zhang & Zhang &
396 Wang & Li & Feng & Zhao & Liu & Qin, 2007b), which may explain the highest
397 average contribution of inorganic particulate matter to $K_d(\text{PAR})$ (71.55%) in the YGR
398 lakes. Most of the studied lakes in YGR, over 60%, was mesotrophic with the lower
399 Chl*a* concentration, except a few highly eutrophic lakes, such as Dianchi Lake and
400 Xingyun Lake. The algae and phytoplankton existed with an appropriate biomass, and
401 pigment particulate matter only had a weak contribution to $K_d(\text{PAR})$. The strong



402 photobleaching and photodegradation by intensive ultraviolet radiation in YGR have
 403 destroyed CDOM structure and weakened CDOM light absorption, resulting in the
 404 minimum contribution to $K_d(\text{PAR})$. The same phenomenon occurred in TQR (Fig. 7).
 405 However, in ER, the relative contributions of Chla to $K_d(\text{PAR})$ is nearly equal to the
 406 inorganic particulate matter. ER situated in the fluvial plains, and most lakes were
 407 shallow (2.8 ± 1.8 m), the waters always have high concentrations of suspended
 408 particulate matter due to the re-suspension of bottom sediments and inflow of surface
 409 runoff (Bachmann et al., 2000; Zhang et al., 2007c). Waters in the ER are highly turbid
 410 with a very low transparency (0.4 ± 0.3 m). Meanwhile, the relatively high
 411 concentrations of nutrients (TN: 0.94 ± 1.31 mg/L, and TP: 0.32 ± 1.02 mg/L) in lakes
 412 resulted in phytoplankton overgrowth, even bloom. 85% of the studied lakes in the ELR
 413 was eutrophic or hyper-eutrophic according to Carlson's trophic index (Carlson, 1977),
 414 the pigment particulate matter during the algae decomposes and metabolism was
 415 released to water. Many studies have proven that the controlling factor of $K_d(\text{PAR})$ was
 416 different with variation of the region (Zheng et al., 2016). Despite Chla and CDOM
 417 contributed to $K_d(\text{PAR})$ in ER and MXR lakes, inorganic particulate matter was largely
 418 responsible for the attenuation. The relationships coefficient and fitting degrees (R^2)
 419 between $K_d(\text{PAR})$ and a_{OACs} all changed in different limnetic regions, which further
 420 veriflicated indicate that the deciding factor of $K_d(\text{PAR})$ was different. This study have
 421 indicated that althouth it sometimes had the same decisiving factor of $K_d(\text{PAR})$ in
 422 different regions, the relative contributions of OACs to $K_d(\text{PAR})$ still had a huge
 423 difference.

424 **4.2 Influence of OACs absorption on $K_d(\text{PAR})$ in lakes**

425 OACs have the deciding effect on $K_d(\text{PAR})$ value (Shi et al., 2014). In this study, either
 426 in five limnetic regions or different trophic lakes, the OACs absorption and $K_d(\text{PAR})$



427 had a significantly positive correlation, a_{OACs} could explain 70%-87% of $K_d(PAR)$
 428 variations (Fig 5, Fig. 8). In the whole study area, a_{NAP} was the most significantly
 429 regulating factor on $K_d(PAR)$. The determination coefficient between $K_d(PAR)$ and a_{NAP}
 430 ($R^2 = 0.79$) was significantly higher than that between $K_d(PAR)$ and a_{phy} , and between
 431 $K_d(PAR)$ and a_{CDOM} ($R^2=0.23$, $R^2=0.16$) (Fig. 4b-d). However, there are marked
 432 differences in the relative contributions of a_{OACs} to light attenuation in different waters
 433 (Belzile et al., 2002; Brandao et al., 2017; Philips & Aldridge & Schelske & Crisman,
 434 1995; V-Balogh et al., 2009).

435 When the lakes were divided into different groups by TSM concentration in this
 436 study, the determining factor of $K_d(PAR)$ changed with the lake type. In the lakes with
 437 low TSM concentration and non-eutrophic lakes with high TSM, a_{CDOM} was the most
 438 powerful factor on $K_d(PAR)$, followed by a_{NAP} . The relative contribution analysis of
 439 CDOM, Chla, and inorganic particulate matters to the total non-water light absorption
 440 was conducted in these waters, and the results indicated that at most of these sampling
 441 waters, CDOM absorption played a major role on total non-water light absorption, and
 442 Chla played a minor role. These waters can be classified as “CDOM-type” water
 443 according to the optical classification of surface waters (Prieur & Sathyendranath,
 444 1981). Studies have indicated that in most of the highly colored inland waters, CDOM
 445 had a dominating influence on light attenuation, reducing the amount of PAR many-
 446 fold (Kirk, 1976; V-Balogh et al., 2009). Besides, the strong correlations between
 447 $K_d(PAR)$ and TSM also implied that light attenuation in the lakes with high TSM
 448 concentration, the particulate absorption, including a_{NAP} and a_{phy} , had an indispensable
 449 influence on $K_d(PAR)$ (Fig. 5). But within the PAR waveband, CDOM absorbs
 450 maximally in the blue region of the spectrum in many natural waters (Frankovich et al.,
 451 2017; Markager & Vincent, 2000; Morris & Zagarese & Williamson & Balseiro &



452 Hargreaves & Modenutti & Moeller & Queimalinos, 1995). CDOM absorption
453 overlaps the blue absorption maximum for Chla, which affected the light availability of
454 phytoplankton, resulting in the low Chla concentration and the low contribution of a_{phy}
455 to $K_d(PAR)$ (Markager & Vincent, 2000).

456 In eutrophic lakes with high TSM, a_{NAP} had the most significant impact on
457 $K_d(PAR)$, followed by a_{phy} . In fact, the low contribution of a_{CDOM} to $K_d(PAR)$ has been
458 predicted since the a_{CDOM} occupied a low proportion in a_{OAC} (Mean \pm SD: $24.30 \pm$
459 14.97%) in this type of lakes. These waters can be classified as “NAP-type” water with
460 high TSM concentrations (Mean \pm SD: 40.94 ± 35.50 mg/L) and high proportion of a_{NAP}
461 to a_{OAC} (Mean \pm SD: $51.19 \pm 22.87\%$) (Prieur & Sathyendranath, 1981). The
462 concentration of calcite particles was the most important factor regulating summer light
463 attenuation within Otisco Lake, New York (Weidemann & Bannister & Effler &
464 Johnson, 1985). In Japan Lake Biwa with bloom-forming cyanobacteria, researchers
465 also found that particulate absorption played significant roles to $K_d(PAR)$ than a_{CDOM}
466 (Belzile et al., 2002). The re-suspension of bottom sediments caused by strong winds
467 in autumn correlated with high $K_d(PAR)$ values, which was because of the high
468 inorganic particles matters concentration (Ma et al., 2016; Song et al., 2017). However,
469 in these turbid waters, the trophic status or Chla concentration also had important
470 influence on light attenuation (Effler et al., 1985). Studies have pointed out that the
471 effect of sediments re-suspension caused by strong wind on $K_d(PAR)$ could be disturbed
472 by the high phytoplankton concentration in spring and summer, the algal bloom in lakes
473 increased the contribution of Chla to $K_d(PAR)$ (Song et al., 2017). The research on
474 hypertrophic waters in Hungary indicated that a_{phy} played an important role in the PAR
475 attenuation (V-Balogh et al., 2009). Results of this study are suggesting that new studies
476 on the variability of $K_d(PAR)$ in inland waters must consider the hydrodynamic



477 conditions, trophic status and the distribution of OACs within the waters (Brandao et
478 al., 2017).

479 The $K_d(\text{PAR})$ in the water is governed by absorption and scattering of water,
480 CDOM, and particulate matter (Ma et al., 2016; Song et al., 2017; Zheng et al., 2016),
481 the pure water effects are always regarded as the background value of $K_d(\text{PAR})$, so the
482 absorption and scattering of OACs have the deciding effect on $K_d(\text{PAR})$ value (Shi et
483 al., 2014). In this study, only the contribution of OACs absorption on $K_d(\text{PAR})$ was
484 analyzed and discussed. The absorption of OACs directly attenuated the photo energy
485 without change of light transmission direction, but the scattering of particles matters
486 changed light transmission direction, which resulted in the change of light absorption
487 along the initial transmission direction (Budhiman et al., 2012; Kirk, 1976; Zheng et al.,
488 2016). In fact, a_{OACs} could explain most of $K_d(\text{PAR})$ variations (Fig 5, Fig. 8), the
489 scattering contribution of particles matters to $K_d(\text{PAR})$ variations in natural waters was
490 relatively small (Belzile et al., 2002; Lund-Hansen, 2004). The previous studies have
491 found that scattering of particles matters decreased approximately linearly with
492 increasing wavelength in particle dominated natural waters (Haltrin, 1999; Morel &
493 Loisel, 1998; Pegau & Zaneveld & Barnard & Maske & Alvarez-Borrego & Lara-Lara
494 & Cervantes-Duarte, 1999). Most of the lakes in this study had the high suspended
495 particles concentration, so the effect of scattering on $K_d(\text{PAR})$ variations may be very
496 weak. Due to the limitation of the our experimental conditions, the scattering of
497 particles matters did not measured in this study, a detailed in situ profiles of spectral
498 absorption and attenuation measured using the AC-9 may help us to understand the
499 results of the research.

500 5. Conclusions

501 The spatial distribution of average $K_d(\text{PAR})$ in five limnetic regions China showed that



the minimum value in TQR (0.60 ± 0.99 and the maximum in NER ($3.17 \pm 2.86 \text{ m}^{-1}$). The inorganic particulate matters had the highest average relative contribution to $K_d(\text{PAR})$ (57.95%).

The a_{OACs} could explain 70%-87% of $K_d(\text{PAR})$ variations with the following relationship: $K_d(\text{PAR}) = 0.41 + 0.57 \times a_{\text{CDOM}} + 0.96 \times a_{\text{NAP}} + 0.57 \times a_{\text{phy}}$ ($R^2 = 0.87$, $n = 741$, $p < 0.001$). However, the influence of different components of a_{OACs} on $K_d(\text{PAR})$ changed with the lake type. In the lakes with low TSM concentration and non-eutrophic lakes with high TSM, a_{CDOM} was the most powerful factor on $K_d(\text{PAR})$. In eutrophic lakes with high TSM, a_{NAP} had the most significant impact on $K_d(\text{PAR})$, followed by a_{phy} . A precise understanding the effect of OACs absorption on $K_d(\text{PAR})$ is essential to remote sensing of water color and evaluate the underwater light climate.

Acknowledgments

This study was jointly supported by the National Natural Science Foundation of China (No. 41730104, No. 41701423), the “One Hundred Talents Program” of the Chinese Academy of Sciences granted to Kaishan Song, 13th Five-Year Plan of Technical and Social Research Project for Jilin Colleges (JJKH20170257KJ), and Jilin Scientific & Technological Development Program (No. 20160520075JH).

References

- APHA, AWWA, WEF: Standard methods for the examination of water and wastewater, American Public Health Association, Washington, 1998.
- Bachmann, R. W., Hoyer, M. V., Canfield, D. E.: The Potential For Wave Disturbance in Shallow Florida Lakes, *Lake Reserv. Manage.*, 16(4), 281-291, 2000.
- Belzile, C., Vincent, W. F., Kumagai, M.: Contribution of absorption and scattering to the attenuation of UV and photosynthetically available radiation in Lake Biwa, *Limnol. Oceanogr.*, 47(1), 95-107, 2002.
- Brandao, L. P. M., Brighenti, L. S., Staehr, P. A., Barbosa, F. A. R., Bezerra-Neto, J. F.: Partitioning of the diffuse attenuation coefficient for photosynthetically available irradiance in a deep dendritic



- 530 tropical lake, *Anais Da Academia Brasileira De Ciencias*, 89(1), 469-489, 2017.
- 531 Bricaud, A., Morel, A., Prieur, L.: Absorption by dissolved organic matter of the sea (Yekkow substance)
532 in the UV and visible domains, *Limnol. Oceanogr.*, 26(1), 43-53, 1981.
- 533 Bricaud, A., Stramski, D.: Spectral absorption coefficients of living phytoplankton and nonalgal
534 biogenous matter: A comparison between the Peru upwelling area and the Sargasso Sea, *Limnol.*
535 *Oceanogr.*, 35(3), 562-582, 1990.
- 536 Budhiman, S., Suhyb Salama, M., Vekerdy, Z., Verhoef, W.: Deriving optical properties of Mahakam
537 Delta coastal waters, Indonesia using in situ measurements and ocean color model inversion,
538 *ISPRS J. Photogramm. Remote Sens.*, 68, 157-169, 2012.
- 539 Carlson, R. E.: A trophic state index for lakes, *Limnol. Oceanogr.*, 22(2), 361-369, 1977.
- 540 Chen, J., Zhu, Y., Wu, Y., Cui, T., Ishizaka, J., Ju, Y.: A Neural Network Model for K(lambda) Retrieval
541 and Application to Global K-par Monitoring, *PLoS One* 10(6), 2015.
- 542 Cleveland, J. S., Weidemann, A. D.: Quantifying absorption by aquatic particles: A multiple scattering
543 correction for glass-fiber filters, *Limnol. Oceanogr.*, 38(6), 1321-1327, 1993.
- 544 Cunningham, A., Ramage, L., McKee, D.: Relationships between inherent optical properties and the
545 depth of penetration of solar radiation in optically complex coastal waters, *J Geophys. Res.-*
546 *Oceans*, 118(5), 2310-2317, 2013.
- 547 Devlin, M. J., Barry, J., Mills, D. K., Gowen, R. J., Foden, J., Sivyver, D., Greenwood, N., Pearce, D.,
548 Tett, P.: Estimating the diffuse attenuation coefficient from optically active constituents in UK
549 marine waters, *Estuar. Coast. Shelf Sci.*, 82(1), 73-83, 2009.
- 550 Devlin, M. J., Barry, J., Mills, D. K., Gowen, R. J., Foden, J., Sivyver, D., Tett, P.: Relationships between
551 suspended particulate material, light attenuation and Secchi depth in UK marine waters, *Estuar.*
552 *Coast. Shelf Sci.*, 79(3), 429-439, 2008.
- 553 Effler, S. W., Schafran, G. C., Driscoll, C. T.: Partitioning Light Attenuation in an Acidic Lake, *Can. J.*
554 *Fish. Aquat. Sci.*, 42(11), 1707-1711, 1985.
- 555 Frankovich, T. A., Rudnick, D. T., Fourqurean, J. W.: Light attenuation in estuarine mangrove lakes,
556 *Estuar. Coastal Shelf Sci.*, 184, 191-201, 2017.
- 557 Haltrin, V. I.: Chlorophyll-based model of seawater optical properties, *Appl. Opt.*, 38(33), 6826-6832,
558 1999.
- 559 James, W. F., Best, E. P., Barko, J. W.: Sediment resuspension and light attenuation in Peoria Lake: can
560 macrophytes improve water quality in this shallow system?, *Hydrobiologia*, 515(1-3), 193-201,
561 2004.
- 562 Jeffrey, S. W., Humphrey, G. F.: New spectrophotometric equations for determining chlorophylls a, b, c1
563 and c2 in higher plants, algae and natural phytoplankton, *Biochemie und Physiologie der*
564 *Pflanzen*, 167(2), 191-194, 1975.
- 565 Jin, X. C., Xu, Q. J., Huang, C. Z.: Current status and future tendency of lake eutrophication in China,
566 *Science in China Series C-Life Sciences*, 48, 948-954, 2005.
- 567 Kirk, J. T. O.: *Light and Photosynthesis in Aquatic Ecosystems*. Cambridge University Press, UK, 1994.
- 568 Kirk, J. T. O.: Yellow substance (gelbstoff) and its contribution to the attenuation of photosynthetically
569 active radiation in some inland and coastal south-eastern Australian waters, *Australian Journal*
570 *of Mar. Freshwater Res.*, 27(1), 61-71, 1976.
- 571 Laurion, I., Ventura, M., Catalan, J., Psenner, R., Sommaruga, R.: Attenuation of ultraviolet radiation in
572 mountain lakes: Factors controlling the among- and within-lake variability, *Limnol. Oceanogr.*,
573 45(6), 1274-1288, 2000.



- 574 Lund-Hansen, L. C.: Diffuse attenuation coefficients $K_d(\text{PAR})$ at the estuarine North Sea-Baltic Sea
575 transition: time-series, partitioning, absorption, and scattering, *Estuar. Coastal Shelf Sci.*, 61(2),
576 251-259, 2004.
- 577 Ma, J., Song, K., Wen, Z., Zhao, Y., Shang, Y., Fang, C., Du, J.: Spatial Distribution of Diffuse
578 Attenuation of Photosynthetic Active Radiation and Its Main Regulating Factors in Inland
579 Waters of Northeast China, *Remote Sens.*, 8(11), 2016.
- 580 Ma, R., Yang, G., Duan, H., Jiang, J., Wang, S., Feng, X., Li, A., Kong, F., Xue, B., Wu, J., Li, S.: China's
581 lakes at present: Number, area and spatial distribution, *Sci. China Earth Sci.*, 41(3), 394-401,
582 2011.
- 583 Markager, S., Vincent, W. F.: Spectral light attenuation and the absorption of UV and blue light in natural
584 waters, *Limnol. Oceanogr.*, 45(3), 642-650, 2000.
- 585 Matsushita, B., Yang, W., Yu, G., Oyama, Y., Yoshimura, K., Fukushima, T.: A hybrid algorithm for
586 estimating the chlorophyll-a concentration across different trophic states in Asian inland waters,
587 *ISPRS J. Photogramm. Remote Sens.*, 102, 28-37, 2015.
- 588 Morel, A., Loisel, H.: Apparent optical properties of oceanic water: dependence on the molecular
589 scattering contribution, *Appl. Opt.*, 37(21), 4765-4776, 1998.
- 590 Morris, D. P., Zagarese, H., Williamson, C. E., Balseiro, E. G., Hargreaves, B. R., Modenutti, B., Moeller,
591 R., Queimalinos, C.: The attenuation of solar UV radiation in lakes and the role of dissolved
592 organic carbon, *Limnol. Oceanogr.*, 40(8), 1381-1391, 1995.
- 593 Ndebele-Murisa, M. R., Musil, C. F., Magadza, C. H. D., Raitt, L.: A decline in the depth of the mixed
594 layer and changes in other physical properties of Lake Kariba's water over the past two decades,
595 *Hydrobiologia*, 721(1), 185-195, 2014.
- 596 Oliver, S. K., Collins, S. M., Soranno, P. A., Wagner, T., Stanley, E. H., Jones, J. R., Stow, C. A., Lottig,
597 N. R.: Unexpected stasis in a changing world: Lake nutrient and chlorophyll trends since 1990,
598 *Global Change Biol.*, 23(12), 5455-5467, 2017.
- 599 Pegau, W. S., Zaneveld, J. R. V., Barnard, A. H., Maske, H., Alvarez-Borrego, S., Lara-Lara, R.,
600 Cervantes-Duarte, R.: Inherent optical properties in the Gulf of California, *Cienc. Mar.*, 25(4),
601 469-485, 1999.
- 602 Philips, E. J., Aldridge, F. J., Schelske, C. L., Crisman, T. L.: Relationships between light availability,
603 chlorophyll-a, and tripton in a large, shallow subtropical lake, *Limnol. Oceanogr.*, 40(2), 416-
604 421, 1995.
- 605 Philips, E. J., Lynch, T. C., Badylak, S.: Chl-a, tripton, color, and light availability in a shallow tropical
606 inner-shelf lagoon, *Mar. Ecol. Prog. Ser.*, 127(1-3), 223-234, 1995.
- 607 Pierson, D. C., Kratzer, S., Strombeck, N., Hakansson, B.: Relationship between the attenuation of
608 downwelling irradiance at 490 nm with the attenuation of PAR (400 nm-700 nm) in the Baltic
609 Sea, *Remote Sens. Environ.*, 112(3), 668-680, 2008.
- 610 Pierson, D. C., Markensten, H., Strömbeck, N.: Long and short term variations in suspended particulate
611 material: the influence on light available to the phytoplankton community. *The Interactions*
612 *between Sediments and Water*, Dordrecht, Springer Netherlands, 299-304, 2003.
- 613 Pope, R. M., Fry, E. S.: Absorption spectrum (380-700 nm) of pure water .2. Integrating cavity
614 measurements, *Appl. Opt.*, 36(33), 8710-8723, 1997.
- 615 Prieur, L., Sathyendranath, S.: An optical classification of coastal and oceanic waters based on the
616 specific spectral absorption curves of phytoplankton pigments, dissolved organic matter, and
617 other particulate materials, *Limnol. Oceanogr.*, 26(4), 671-689, 1981.



- 618 Raymond, P. A., Hartmann, J., Lauerwald, R., Sobek, S., McDonald, C., Hoover, M., Butman, D., Striegl,
619 R., Mayorga, E., Humborg, C., Kortelainen, P., Duerr, H., Meybeck, M., Ciais, P., Guth, P.:
620 Global carbon dioxide emissions from inland waters, *Nature*, 503(7476), 355-359, 2013.
- 621 Shang, Y., Song, K., Wen, Z., Lyu, L., Zhao, Y., Fang, C., Zhang, B.: Characterization of CDOM
622 absorption of reservoirs with its linkage of regions and ages across China, *Environ. Sci. Pollut.*
623 *Res.*, 2018.
- 624 Shi, K., Zhang, Y., Liu, X., Wang, M., Qin, B.: Remote sensing of diffuse attenuation coefficient of
625 photosynthetically active radiation in Lake Taihu using MERIS data, *Remote Sens. Environ.*,
626 140, 365-377, 2014.
- 627 Song, K., Ma, J., Wen, Z., Fang, C., Shang, Y., Zhao, Y., Wang, M., Du, J.: Remote estimation of K-d
628 (PAR) using MODIS and Landsat imagery for turbid inland waters in Northeast China, *ISPRS*
629 *J. Photogramm. Remote Sens.*, 123, 159-172, 2017.
- 630 Song, K., Wen, Z., Shang, Y., Yang, H., Lyu, L., Liu, G., Fang, C., Du, J., Zhao, Y.: Quantification of
631 dissolved organic carbon (DOC) storage in lakes and reservoirs of mainland China, *J. Environ.*
632 *Manage.*, 217, 391-402, 2018.
- 633 Song, K. S., Zang, S. Y., Zhao, Y., Li, L., Du, J., Zhang, N. N., Wang, X. D., Shao, T. T., Guan, Y., Liu,
634 L.: Spatiotemporal characterization of dissolved carbon for inland waters in semi-humid/semi-
635 arid region, China, *Hydrol. Earth Syst. Sci.*, 17(10), 4269-4281, 2013.
- 636 Stambler, N.: Bio-optical properties of the northern Red Sea and the Gulf of Eilat (Aqaba) during winter
637 1999, *J. Sea Res.*, 54(3), 186-203, 2005.
- 638 V-Balogh, K., Nemeth, B., Voros, L.: Specific attenuation coefficients of optically active substances and
639 their contribution to the underwater ultraviolet and visible light climate in shallow lakes and
640 ponds, *Hydrobiologia*, 632(1), 91-105, 2009.
- 641 Van Duin, E. H. S., Blom, G., Los, F. J., Maffione, R., Zimmerman, R., Cerco, C. F., Dortch, M., Best,
642 E. P. H.: Modeling underwater light climate in relation to sedimentation, resuspension, water
643 quality and autotrophic growth, *Hydrobiologia*, 444(1), 25-42, 2001.
- 644 Weidemann, A. D., Bannister, T. T., Effler, S. W., Johnson, D. L.: Particulate and optical properties during
645 CaCO₃ precipitation in Otisco Lake, *Limnol. Oceanogr.*, 30(5), 1078-1083, 1985.
- 646 Wen, Z., Song, K., Shang, Y., Fang, C., Li, L., Lv, L., Lv, X., Chen, L.: Carbon dioxide emissions from
647 lakes and reservoirs of China: A regional estimate based on the calculated pCO₂, *Atmos.*
648 *Environ.*, 170(Supplement C), 71-81, 2017.
- 649 Wen, Z. D., Song, K. S., Zhao, Y., Du, J., Ma, J. H.: Influence of environmental factors on spectral
650 characteristics of chromophoric dissolved organic matter (CDOM) in Inner Mongolia Plateau,
651 China, *Hydrol. Earth Syst. Sci.*, 20(2), 787-801, 2016.
- 652 Wetzel, R. G.: *Limnology: Lake and River Ecosystems*, Third Edition ed. Academic Press, California,
653 USA, 2001.
- 654 Yamaguchi, H., Katahira, R., Ichimi, K., Tada, K.: Optically active components and light attenuation in
655 an offshore station of Harima Sound, eastern Seto Inland Sea, Japan, *Hydrobiologia*, 714(1),
656 49-59, 2013.
- 657 Yang, H., Xie, P., Xing, Y. P., Ni, L. Y., Guo, H. T.: Attenuation of photosynthetically available radiation
658 by chlorophyll, chromophoric dissolved organic matter, and tripton in lake Donghu, China, *J.*
659 *Freshwat. Ecol.*, 20(3), 575-581, 2005.
- 660 Zhang, Y., Zhang, B., Ma, R., Feng, S., Le, C.: Optically active substances and their contributions to the
661 underwater light climate in Lake Taihu, a large shallow lake in China, *Fund. Appl. Limnol.*,



- 662 170(1), 11-19, 2007a.
- 663 Zhang, Y., Zhang, B., Wang, X., Li, J., Feng, S., Zhao, Q., Liu, M., Qin, B.: A study of absorption
664 characteristics of chromophoric dissolved organic matter and particles in Lake Taihu, China,
665 *Hydrobiologia*, 592, 105-120, 2007b.
- 666 Zhang, Y., Zhou, Y., Shi, K., Qin, B., Yao, X., Zhang, Y.: Optical properties and composition changes in
667 chromophoric dissolved organic matter along trophic gradients: Implications for monitoring and
668 assessing lake eutrophication, *Water Res.*, 131, 255-263, 2018.
- 669 Zhang, Y. L., Zhang, B., Ma, R. H., Feng, S., Le, C. F.: Optically active substances and their contributions
670 to the underwater light climate in Lake Taihu, a large shallow lake in China, *Fund. Appl.*
671 *Limnol.*, 170(1), 11-19, 2007c.
- 672 Zhao, Y., Song, K., Wen, Z., Li, L., Zang, S., Shao, T., Li, S., Du, J.: Seasonal characterization of CDOM
673 for lakes in semiarid regions of Northeast China using excitation–emission matrix fluorescence
674 and parallel factor analysis (EEM–PARAFAC), *Biogeosciences*, 13(5), 1635-1645, 2016.
- 675 Zheng, Z., Ren, J., Li, Y., Huang, C., Liu, G., Du, C., Lyu, H.: Remote sensing of diffuse attenuation
676 coefficient patterns from Landsat 8 OLI imagery of turbid inland waters: A case study of
677 Dongting Lake, *Sci. Total Environ.*, 573, 39-54, 2016.
- 678